www.sciencemag.org/content/349/6249/742/suppl/DC1

Supplementary Material for

Mus81 and converging forks limit the mutagenicity of replication fork breakage

Ryan Mayle, Ian M. Campbell, Christine R. Beck, Yang Yu, Marenda Wilson, Chad A. Shaw, Lotte Bjergbaek, James R. Lupski, Grzegorz Ira*

*Corresponding author. E-mail: gira@bcm.edu

Published 14 August 2015, *Science* **349**, 742 (2015)
DOI: 10.1126/science.aaa8391

This PDF file includes:

Supplementary Materials

Materials and Methods

Flp-nickase induced broken fork recombination assay. Single ended DSBs were induced by a GAL10-Flp1H305L step arrest mutant of the Flp1 recombinase, which makes a nick at an FRT site, but stays covalently linked to the 3' side of the nick as it is unable to complete the ligation portion of the enzymatic reaction. An FRT site was inserted at three genomic locations. 1) ChrII at nucleotide 23,700, between ARS202, the most centromere distal efficient origin, and the telomere. 2) ChrIV at nucleotide 1,493,950, between ARS442, the most centromere distal efficient origin, and the telomere. 3) ChrVI at nucleotide 196,500, between ARS606 and ARS607. While additional origins exist between the FRT and the telomere on ChrII and ChrIV, all are either low efficiency, dormant, or unconfirmed. Viability of cells upon Flp induction was assayed by plating on YP-Galactose and comparing growth to the same strain on YP-Glucose. An overnight YPD culture was used to inoculate a 5 mL YP-Raffinose culture, which was incubated at 30ºC for 6 hrs, to a concentration of $1x10^7$ cells/mL. 10-fold serial dilutions were then plated on YP-Glucose and YP-Galactose plates. Plates were then imaged after 2 days at 30ºC to assess viability qualitatively in response to fork breakage. Recombination deficient *rad52* mutant was used as negative control. As recombination between sister chromatids restores the original FRT sequence, cells continue to undergo cleavage and repair throughout colony formation. As an additional way of observing growth defects, cells were grown as above and ~100 cells were plated on YP-Glucose and YP-Galactose. Plates were grown at 30ºC and imaged every day from 2-6 days after plating.

Analysis of seDSB formation. YP-Raffinose cultures were inoculated from overnight YP-Glucose starter cultures and grown at 30ºC to a concentration of $1x10^7$ cells/mL. The FLP-nickase was then induced by adding galactose at a final concentration of 2%, and cells were collected at 0 hrs, 2 hrs, and 4 hrs. Following DNA isolation via glass-beads and phenol/chloroform extraction and ethanol precipitation, samples were digested with the restriction enzyme *Acc*I. Digested DNA was separated by gel electrophoresis in 0.8% agarose, then transferred to a membrane for Southern blotting. Probes specific to sequences on either side of the FRT were used to confirm that seDSB were generated at FRTs. The fact that the stronger bands are those corresponding to probes specific for sequences between the FRT and the nearby efficient origin of replication (Probe A) indicate that breaks are predominantly single ended and originate from the efficient origin side of the break. The weak band observed for Probe B at each position could correspond to rare two ended breaks and/or infrequent breakage originating from the opposite side of the FRT. The percentage of seDSBs was calculated as the normalized signal intensity of the "cut" band corresponding to the sequences between origin of replication and FRT divided by the sum of the normalized intensities of both cut bands.

Estimation of 5-FOA^R rates. URA3 reporters were inserted at different distances from FRT loci as indicated in Figure 2. For ChrVI, 2 kb is at position 196,850, 5 kb at 193,945,

and 17 kb at 181,500. For ChrIV, 8 kb is at 1,501,100, and 17 kb at 1,510,000. For ChrII, 7 kb is at position 18,550, and 15 kb at 9,850. Inactivation or loss of the *URA3* reporter was followed on 5-FOA plates. Overnight YPD starter cultures were used to inoculate YP-Raffinose cultures, which were grown to $1x10^7$ cell/mL before plating 20-30 cells per plate on YP-Galactose media. Plates were incubated at 30ºC for 6 days to allow colonies to grow. For each strain tested, 30 individual colonies were plated on 5-FOA plates. To control for the number of cells plated, a small aliquot was taken and plated on rich medium. 5-FOA plates were incubated at 30ºC for 2 days, at which point 5-FOA^R colonies were counted, and mutation rates were estimated as described below.

Because the *mus81*Δ *yen1*Δ double mutant has a repair defect (**Fig. 1c**), rates for these strains were corrected based on the relative viability of these strains on Galactose compared to wild type. We estimated, that ~50% of cells in *mus81*Δ*yen1*Δ mutant colonies are dead relative to about <10% in wild type cells, thus a correction factor of 2x was used to correct the rates calculated for all *mus81*Δ*yen1*Δ strains. This is likely an underestimation, as not every cell in a population has a nick induced DSB. Thus colonies in repair deficient mutants can be formed from cells that did not undergo DNA breakage/repair. Nearly all mutants tested eventually form colonies on YEP-GAL plates, including recombination deficient *rad52* cells. The exception is the *mus81yen1* mutant with the fork breakage at chromosome VI (between two efficient origins of replication), which forms only very small colonies, thus precluding mutation analysis (**Fig. S3**).

Statistical analysis. To perform statistical comparison of mutation rates between genotypes, we utilized the Drake estimator of mutation rate {Drake, 1991 #1111} and adapted a bootstrap resampling approach {Russell, 2011 #1112} to determine p-values for comparisons between genotypes. The Drake estimator is defined:

$$\mu = \frac{m/N}{\ln(\mu N)}$$

where μ is the estimated mutation rate, m is the median number of mutants observed across observations, and N is the mean number of cells plated. This non-linear equation can be solved using a quasi Newton-Raphson method root finder; we utilized one such method as implemented in the R Statistical Programing Language function uniroot. Briefly, this method requires an implementation of the estimator equation, an initial starting estimate and a tolerance for determining convergence. The method iteratively searches for a solution to the non-linear equation and halts when its solution is within the tolerance.

The null hypothesis in our analysis is that mutation rates are equivalent between genotypes. To perform bootstrap resampling to generate a p-value for comparing genotype pairs, we implemented a procedure to draw two samples with replacement from the pooled collection of data for the pairs under consideration. We then computed the Drake estimated mutation rate for each bootstrap sample, and we calculated the difference between the pair of mutation rate estimate. We repeated this procedure 10,000 times and computed the empirical distribution of the absolute value of these differences.

We then determined the p-value by calculating one minus the empirical percentile of the absolute value of the observed difference as calculated from the real data. We repeated this procedure for each pair of genotypes. To account for the multiple genotype comparisons being performed, we used the Holm method to compute adjusted p-values.

To estimate the standard deviation of the mutation rate for each individual genotype, we performed within genotype bootstrap resampling, recalculating the Drake mutation rate estimate for each resample. We determined the standard deviation of these resampled estimates.

Determination of sequence changes for 5-FOA^R mutants. 5-FOA^R mutants were streaked on 5-FOA containing plates to obtain purified single colonies. A single colony for each mutant was then patched to a YPD plate, and genomic DNA was isolated. The *ura3* reporter was then amplified using primers 300-500 bp upstream and downstream of the reporter insertion site, as described below, and sequenced using primers 20 bp upstream of the start codon (CGAAGATAAATCATGTCGAAAGC) and 20 bp downstream of the stop codon (TGGCCGCATCTTCTCAAATA) in order to identify coding sequence changes. Nucleotide changes were determined by alignment with the wild type *URA3* sequence. Primers used to amplify the reporter gene are as follows: On ChrII, TTTCATGCTGTTGGGCAGGA and TAAAACCCTGCGAGTTCTGCT for 0.2 kb, and ATAAGCCAAAAAGCGGCTCA and CGAACTGGCAAATACGGAAT for 15 kb. On ChrVI, TCCCCATCAAAGTTACATCG and TGCATGGGTTCGTTAATCGA for 0.2 kb, and AATACCTGTAAATAGCCCCGC and ACAAACAACCCGAGACAAGA for 17 kb. On ChrIV, TGGCTTTCTTTTCCTCTAACG and TTTTCCATTTCAGCTAACGTG for 0.2 kb.

Mutants for which *ura3* could not be amplified were classified as GCRs. Events where PCR fragments was larger or smaller were classified as duplications or deletions. As small duplications/deletions are very rare, they are not presented as a separate category but are instead added to GCRs. However deletions and duplications are listed separately in **Table S1.**

Analysis of GCR events. GCRs were analyzed in detail at several reporter positions where the rate of GCRs is highest, all in the presence of the *ura3-1* allele on ChrV. The highest rate of GCRs in wild type cells was observed at *URA3* reporter positions close to the broken fork (0.2 kb) on ChrII and ChrVI in wild type cells, and 15 kb from the break on ChrII in *mus81*Δ cells. PCR, sequencing, chromosomal analysis by CHEF and Southern blotting were utilized to determine the most common types of rearrangements at each of these locations. Using multiple sets of primers specific for sequences around the *URA3* reporters, we found that sequences between the reporter on one side of the FRT and a Ty or Ty LTR on the opposite side of the FRT are missing in GCRs for reporter positions 0.2 kb on both ChrVI and ChrII. Analysis of chromosome size by pulse field gel electrophoresis followed by Southern blotting showed an increase in size for the chromosome carrying the FRT. Agarose plugs containing yeast chromosomes were subjected to electrophoresis using a CHEF DRII with an initial pulse time of 60s and final pulse time of 90s at 6V/cm for 24 hours. Southern blot analysis was performed

using probes specific to regions between the *URA3* reporter and a Ty or Ty LTRs on chromosomes carrying the FRT (ChrVI or ChrII), or between *ura3-1* and Ty LTR on ChrV. As shown in extended data figures 4 and 5, sequences between the *URA3* reporter and a Ty or Ty LTR on either ChrII or ChrVI respectively were replaced with sequences between *ura3-1* and a corresponding Ty LTR on ChrV. Additional probes on ChrII or ChrVI, as well as on ChrV just outside the region flanked by *ura3-1* and the LTRs, confirmed the nature of these deletion/insertion events. Rearrangements were also confirmed by PCR using primers on either side of all junctions, where a PCR product is only generated in cells carrying these rearrangements. The following primers were used to monitor junctions: for Ty junctions between ChrII and ChrV, GGCTATTTGAAAATTTGTTTAGG on ChrV and TTGGTACTGTCCATTCTGTGGA or AGAGAGGGAGTAACAACGTCAATG for the 5' or 3' LTR on ChrII respectively. For Ty junction between ChrVI and ChrV, TTCCATCCTACAAACAGCTACAGC on ChrV and ATGGACCTCCTGAGTCATTGA on ChrV. For *URA3* junctions, GCGATACAGAAAGAAAAAAGCG on ChrV, and TCCAATAGATATAGACACATCCGA or TTTCATGCTGTTGGGCAGGA on ChrVI and ChrII respectively. For single template switches between ChrII and ChrV, TAAAACCCTGCGAGTTCTGCT on ChrII and GCAGATAAGTGAATTTGCAGTGG on ChrV. PCR products amplifying Ty LTR junctions were sequenced to identify the location of breakpoints from ChrII or ChrVI to ChrV. This sequencing revealed that these events are mediated by micro homology of 4-26 base pairs. Sequencing of *ura3* junctions confirmed conversion of *URA3* to *ura3-1* as the component of these events conferring resistance to 5-FOA.

Alu mediated template switch assay. Two *Alus* were inserted in the same orientation on ChrII, either 1.2 kb or 9.7 kb from the FRT, marked by *TRP1* and *URA3* respectively, with both markers located between the two *Alus*. These *Alus* are highly divergent, with only 88.2% identity. Each was amplified from the *SPAST* locus of the human genome along with a small amount of flanking unique sequence from chr2:32378354-32378728 (*Alu*Sx1) or chr2:32380880-32381483 (*Alu*Sp) of hg19/GRCh37. Both elements were previously shown to mediate two or more deletions causative of autosomal dominant spastic paraplegia type 4 {Boone, 2014 #1099}. The *Alu* repeats were inserted into the same side of the FRT, and template switches between the two *Alus* during repair causes deletion of the sequences between them, resulting in 5-FOA^R trp- colonies. Mutation rate assays were performed as outlined above, and purified 5-FOA^R colonies were screened for *Alu* mediated deletions using PCR with the primers below, located just outside each *Alu* in unique human genomic sequence. Fusion *Alus* from these deletion events were then sequenced to determine the location of breakpoints, using the following primers: F - GGTCATTTATGCCAAACTGC and R - GGCTACAAACAGCATATGATCC.

Strains and plasmids. All strains were constructed by transformation or cross. The following derivatives of the W303 strain RM019 (*leu2*Δ*1::LEU2-GAL10-FlpH305L, MAT***a***, ade2-1, trp1-1, his3-11, -15, ura3-1, leu2-3, -112, can1-100)* were constructed:

RM005: *FRT-KanMX-ChrVI;* and its derivatives;
- RM001: *mus81::NatMX*; RM002: *yen1::NatMX*; RM006: *rad51::NATMX*; RM007:

yen1::NatMX, *mus81::TRP1*; RM003: *pol32::NatMX*; RM004: *pif1-m2*; RM130: *yen1::NatMX, mus81::TRP1, pol32::KanMX*; RM061: *rad52::NatMX;* RM372: *rad51::NATMX*, *mus81::TRP1;* RM382: *yen1::NATMX*, *rad51::KANMX;* RM373: *yen1::NATMX*, *rad51::KANMX*, *mus81::TRP1*

- RM095: *kanmx::URA3-0.2 kb,* and its derivatives;

RM149: *mus81::TRP1;* RM151: *yen1::NatMX;* RM156: *ura3-1::HphMX;* RM158: *mus81::TRP1, ura3-1::HphMX;* RM160: *yen1::NatMX, ura3-1::HphMX;* RM336: *mus81::TRP1*, *pol32::KANMX*

- RM089: *URA3-2 kb;* and its derivatives;

RM254: *mus81::TRP1*; RM298: *yen1::NatMX;* RM252: *ura3-1::HphMX;* RM271: *mus81::TRP1, ura3-1::HphMX;* RM299: *yen1::NatMX, ura3-1::HphMX*

- RM088: *URA3-5 kb;* and its derivatives;

RM143: *mus81::TRP1*; RM145: *yen1::NatMX;* RM172: *ura3-1::HphMX;* RM174: *mus81::TRP1, ura3-1::HphMX;* RM297: *yen1::NatMX, ura3-1::HphMX*

- RM090: *URA3-17 kb;* and its derivatives;

RM137: *mus81::TRP1*; RM139: *yen1::NatMX;* RM162: *ura3-1::HphMX;* RM164: *mus81::TRP1, ura3-1::HphMX;* RM166: *yen1::NatMX, ura3-1::HphMX*

RM074: *FRT-NatMX-ChrIV;* and its derivatives;

- RM077: *mus81::TRP1*, RM078: *yen1::NatMX*; RM082: *yen1::NatMX, mus81::TRP1*; RM079: *pol32::KanMX*; RM080: *pif1-m2*; RM094: *yen1::NatMX, mus81::TRP1, pol32::KanMX*; RM081: *rad52::KanMX*
- RM108: *NatMX::URA3-0.2 kb;* and its derivatives;

RM131: *mus81::TRP1*; RM133: *yen1::NatMX*; RM128: *yen1::NatMX, mus81::TRP1;* RM176: *ura3-1::HphMX;* RM178: *mus81::TRP1, ura3-1::HphMX;* RM180: *yen1::NatMX, ura3-1::HphMX;* RM182: *mus81::TRP1, yen1::NatMX, ura3-1::HphMX,*

- RM110: *URA3-8 kb,* RM194: *URA3-8 kb, ura3-1::HphMX*
- RM112: *URA3-17 kb,* and its derivatives;

RM124: *mus81::TRP1*; RM126: *yen1::NatMX*; RM122: *mus81::TRP1, yen1::NatMX;* RM186: *ura3-1::HphMX;* RM188: *mus81::TRP1, ura3-1::HphMX;* RM190: *yen::NatMX, ura3-1::HphMX;* RM192: *mus81::TRP1, yen1::NatMX, ura3-1::HphMX*

RM101*: FRT-NatMX-ChrII,* and its derivatives:

- RM102: *mus81::TRP1*; RM103: *yen1::NatMX*; RM106: *yen1::NatMX, mus81::TRP1*; RM104: *pol32::KanMX*; RM105: *pif1-m2;* RM281: *yen1::NatMX, mus81::TRP1, pol32::KanMX*, *URA3-15 kb*; RM107: *rad52::KanMX*; RM311: *FRT-NatMX-ChrII, Alu-URA3, Alu-TRP1;* RM312: *FRT-NatMX-ChrII, Alu-URA3, Alu-TRP1, mus81::TRP1;* RM368: *yen1::NATMX*, *rad51::KANMX*; RM369: *yen1::NATMX*, *rad51::KANMX*, *mus81::TRP1*
- RM219: *NatMX::URA3-0.2 kb;* and it's derivatives;

RM221: *mus81::TRP1*; RM223: *yen1::NatMX*; RM225: *yen1::NatMX*, *mus81::TRP1*; RM240: *pol32::KanMX*; RM246: *pol32::KanMX, mus81::TRP1*; RM256: *rev3::NatMX;* RM228: *ura3-1::HphMX;* RM230: *mus81::TRP1, ura3-1::HphMX;* RM232: *yen1::NatMX, ura3-1::HphMX;* RM234: *yen1::NatMX, mus81::TRP1, ura3-1::HphMX;*

RM243: *pol32::KanMX, ura3-1::HphMX;* RM249: *pol32::KanMX, mus81::TRP1, ura3-1::HphMX*; RM279: *rev3::KanMX, ura3-1::HphMX,* RM330: *rad51::KANMX*; RM333: *rad51::KANMX*, *mus81::TRP1*;

- RM255: *URA3-7 kb;* and its derivatives;

RM257: *mus81::TRP1*; RM300: *yen1::KanMX*; RM301: *yen1::KanMX, mus81::TRP1*; RM258: *pol32::KanMX*; RM267: *pol32::KanMX, mus81::TRP1*; RM295: *rev3::KanMX,* RM264: *ura3-1::HphMX,* RM265: *mus81::TRP1, ura3-1::HphMX*; RM303: *yen1::KanMX, ura3-1::HphMX*; RM302: *yen1::KanMX, mus81::TRP1, ura3-1::HphMX*; RM266: *pol32::KanMX, ura3-1::HphMX*; RM268: *pol32::KanMX*, *mus81::TRP1, ura3-1::HphMX;* RM296: *rev3::KanMX, ura3-1::HphMX*

- RM203: *URA3-15 kb;* and its derivatives;

RM205: *mus81::TRP1;* RM207: *yen1::NatMX*; RM209: *yen1::KanMX*, *mus81::TRP1;* RM242: *pol32::KanMX*; RM248: *pol32::KanMX, mus81::TRP1;* RM278: *rev3::NatMX;* RM211: *ura3-1::HphMX*; RM213: *mus81::TRP1, ura3-1::HphMX*; RM215: *yen1::NatMX, ura3-1::HphMX*; RM217: *yen1::NatMX, mus81::TRP1, ura3-1::HphMX*; RM245: *pol32::KanMX, ura3-1::HphMX*; RM251: *pol32::KanMX, mus81::TRP1, ura3-1::HphMX;* RM280: *rev3::KanMX, ura3-1::HphMX*

The following control strains without FLP, derivatives of the wild type W303 strain *, ade2-1, trp1-1, his3-11, -15, ura3-1, leu2-3, -112, can1-100,* were constructed:

- RM096: *FRT-KanMX-ChrVI, kanmx::URA3-0.2 kb;* RM092*: FRT-KanMX-ChrVI, URA3-2kb;* RM091: *FRT-KanMX-ChrVI, URA3-5kb;* RM093: *FRT-KanMX-ChrVI, URA3-17kb;* RM157: *FRT-KanMX-ChrVI, kanmx::URA3-0.2 kb, ura3-1::HphMX;* RM253*: FRT-KanMX-ChrVI, URA3-2kb, ura3-1::HphMX;* RM173*: FRT-KanMX-ChrVI, URA3-5kb, ura3-1::HphMX;* RM163: *FRT-KanMX-ChrVI, URA3-17kb, ura3-1::HphMX;* RM109: *FRT-NatMX-ChrIV, NatMX::URA3-0.2 kb;* RM111: *FRT-NatMX-ChrIV, URA3-7kb;* RM113*: FRT-NatMX-ChrIV, URA3-17kb;* RM177*: FRT-NatMX-ChrIV, natmx::URA3-0.2 kb, ura3-1::HphMX;* RM195*: FRT-NatMX-ChrIV, URA3-7kb, ura3-1::HphMX;* RM187*: FRT-NatMX-ChrIV, URA3-17kb, ura3-1::HphMX;* RM288*: FRT-NatMX-ChrII, URA3-7kb;* RM204*: FRT-NatMX-ChrII, URA3-15kb;* RM229*: FRT-NatMX-ChrII, NatMX::URA3-0.2 kb, ura3-1::HphMX;* RM289*: FRT-NatMX-ChrII, URA3-7kb, ura3-1::HphMX;* RM212*: FRT-NatMX-ChrII, URA3-15kb, ura3-1::HphMX;* RM313: *FRT-NatMX-ChrII, Alu-URA3, Alu-TRP1;* RM314: *FRT-NatMX-ChrII, Alu-URA3, Alu-TRP1, mus81::TRP1*

- RM220*: FRT-NatMX-ChrII, NatMX::URA3-0.2 kb;* and its derivatives;

RM222: *mus81::TRP1*; RM224: *yen1::NatMX*; RM226: *mus81::TRP1*, *yen1::KanMX*; RM241: *pol32::KanMX*; RM247: *mus81::TRP1*, *pol32::KanMX*; RM290 *rev3::KanMX;* RM343: rad51::KANMX; RM344: *rad51::KANMX*, *mus81::TRP1*

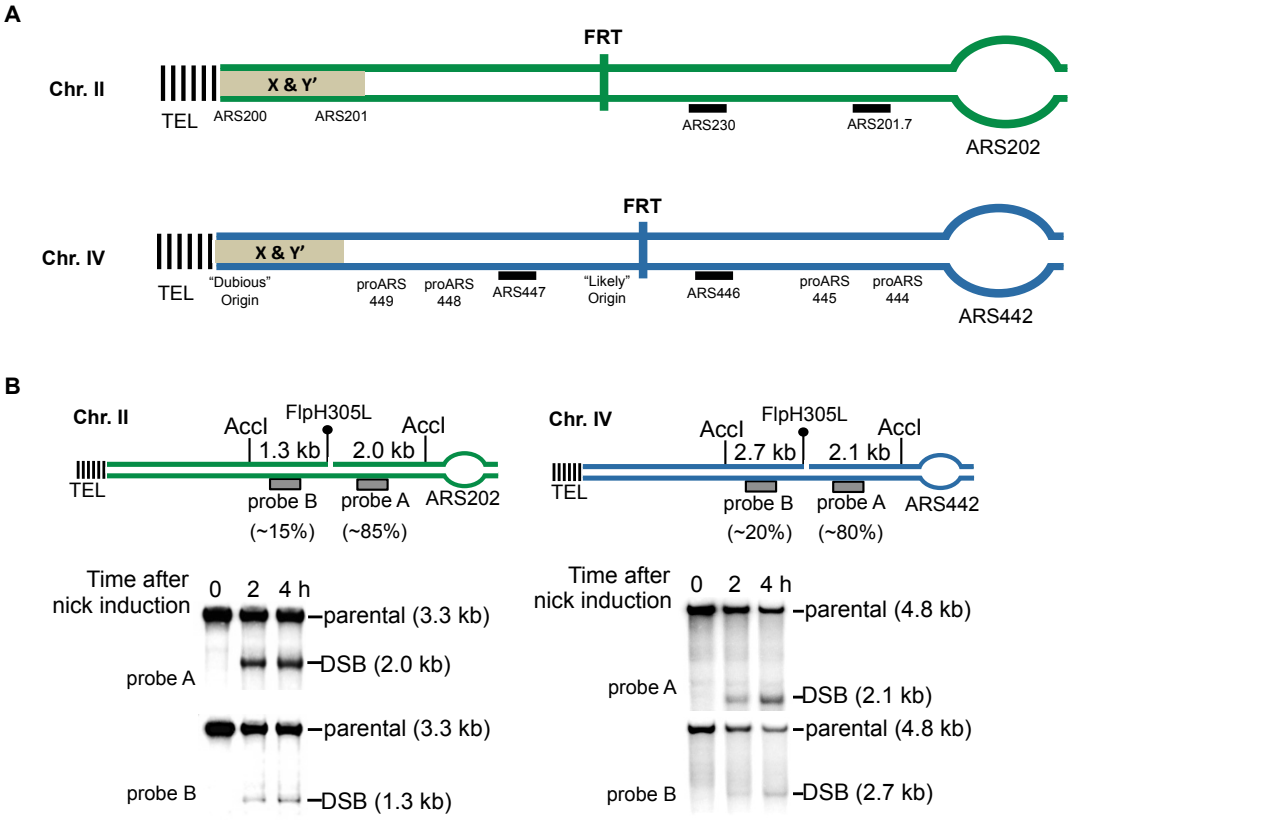

Fig. S1. Analysis of replication fork breakage at subtelomeric positions
A. Diagram showing the location of subtelomeric FRTs on ChrII and ChrIV. All functional and predicted origins (ARS) are shown. Bubbles indicate the closest high efficiency origin, and black bars indicate low efficiency origins. Origins indicated without a bar are either unconfirmed, and/or were not detected by curated timing study or analysis of leading and lagging strand synthesis (*11, 12, 29-31*). **B.** Southern blots showing seDSBs formed on ChrII and ChrIV following Flp-nickase induction. Approximate relative intensities of each DSB band are indicated below the position of the corresponding probe.

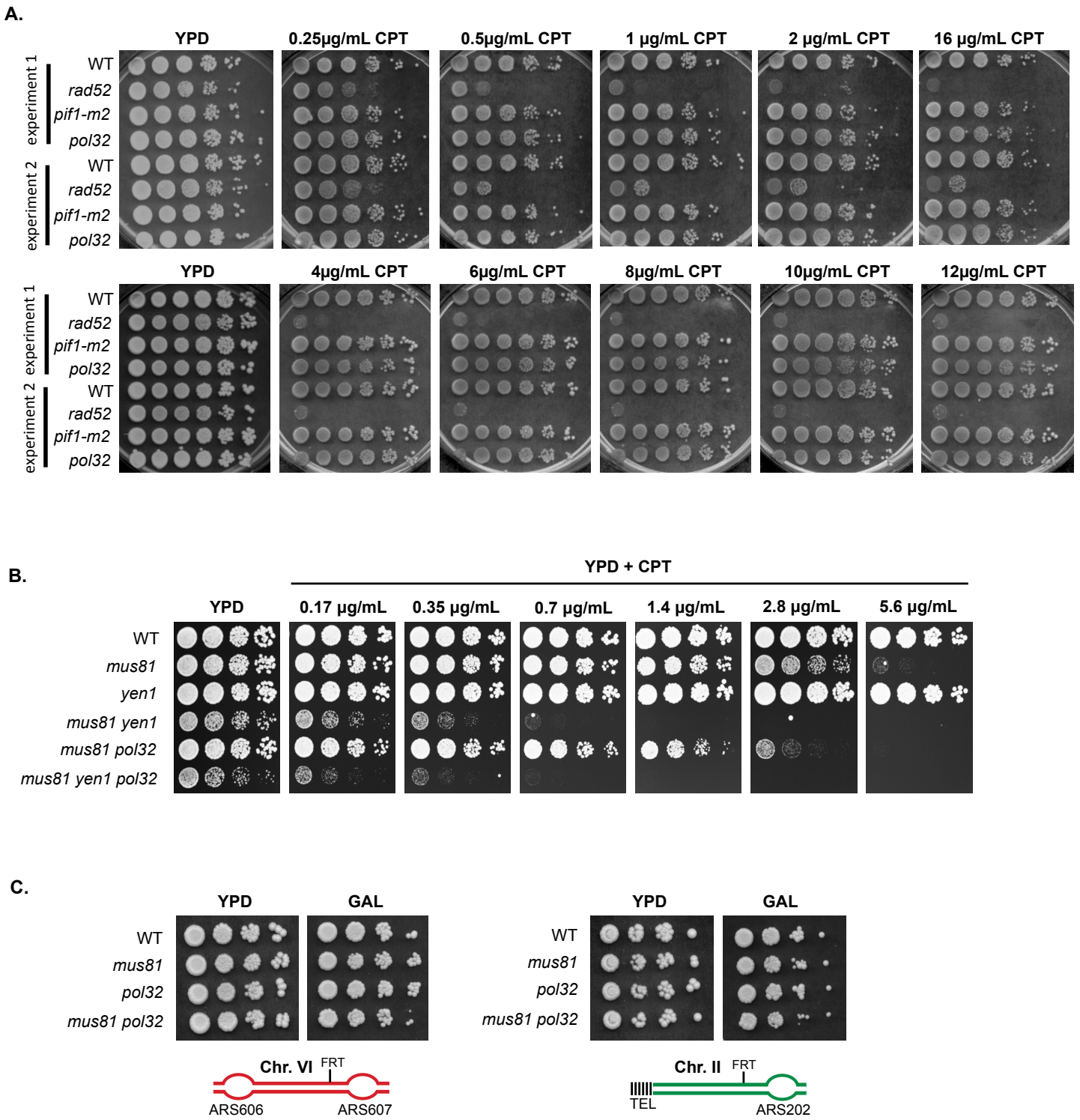

Fig. S2. Role of Pol32 in repair of broken forks and resistance to Camptothecin
A-B. Serial 5-fold dilutions of wild type and indicated mutant strains plated on YPD plates containing a range of Camptothecin (CPT) concentrations. **C**. 10-fold serial dilutions of wild type and mutant strains plated on YPD and YP-GAL. Position of the FRT analyzed is indicated.

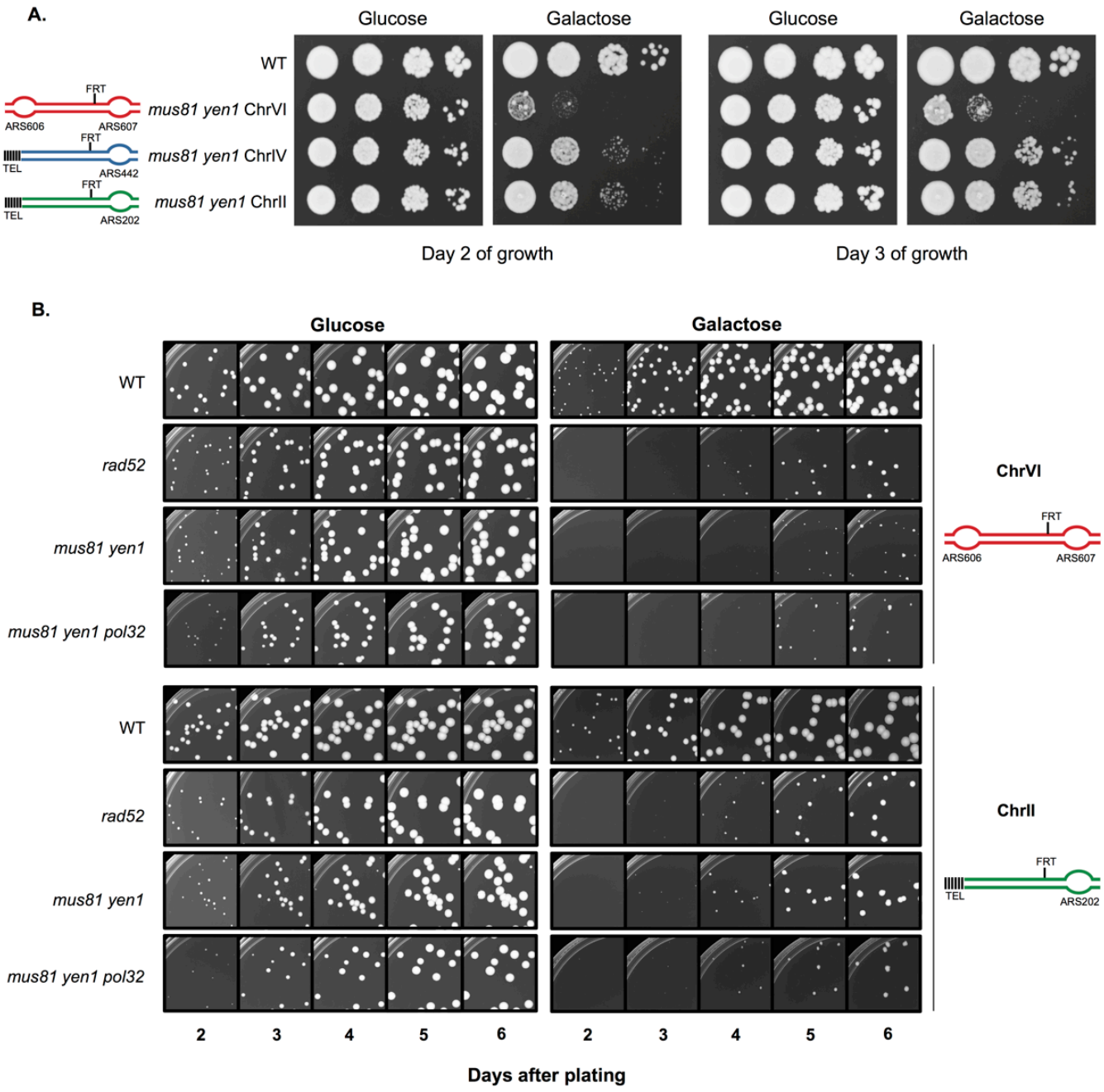

Fig. S3. **The repair defect in *mus81 yen1* cells is less severe for subtelomeric breaks**
A. Serial 10-fold dilutions of wild type and *mus81 yen1* strains plated on YPD and YP-GAL. **B.** Colony formation from 2 to 6 days of growth for wild type and mutant strains plated on YPD and YP-GAL.

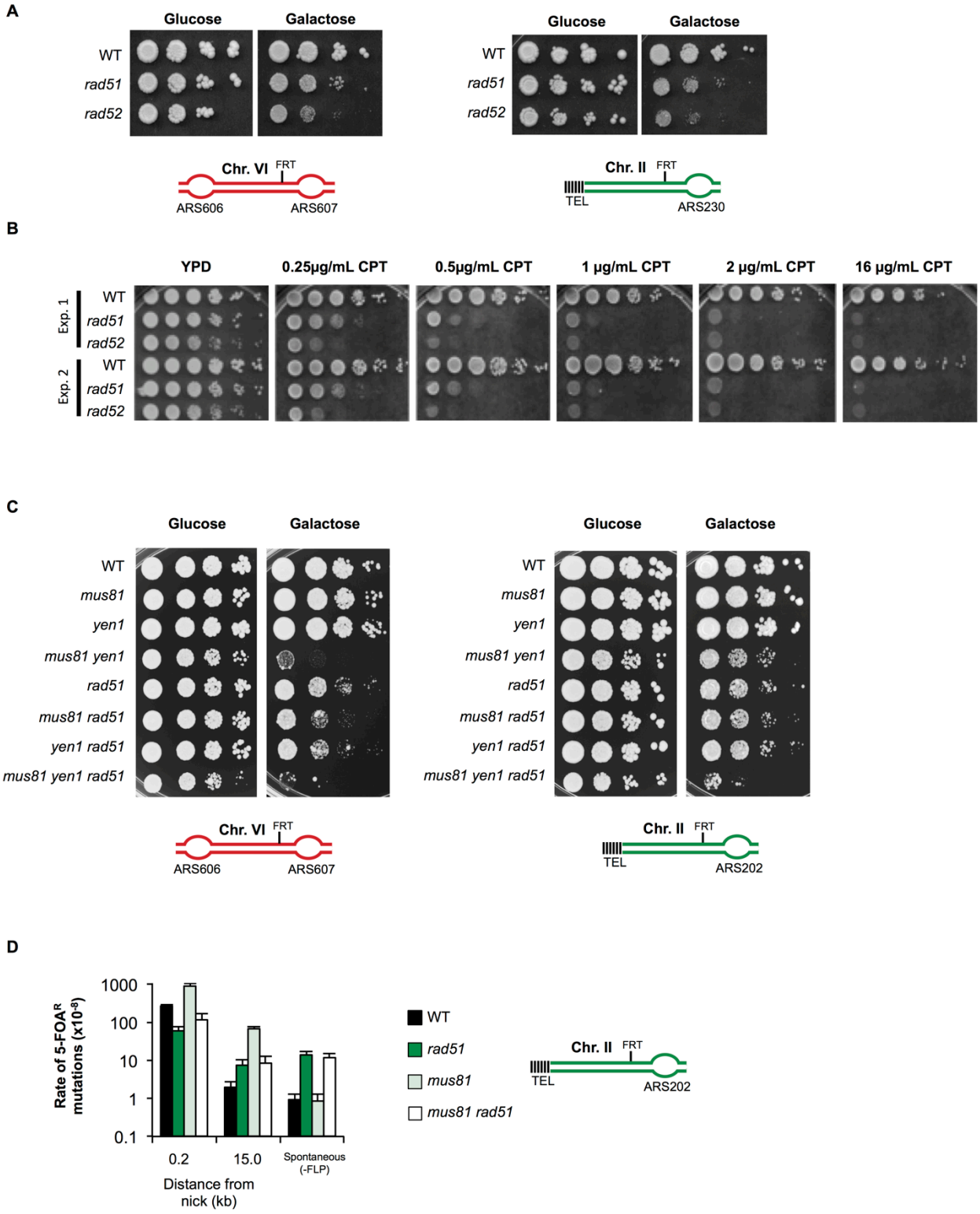

Fig. S4. Repair and mutagenesis at broken forks depend on Rad51

A-C. Serial 10-fold (A,C) or 5-fold (B) dilutions of wild type and mutant strains on YPD and YP-GAL (A,C), or a range of CPT concentrations (B). **D**. Fork breakage induced and spontaneous 5-FOA^R mutation rates for WT and indicated mutant strains. Error bars represent one standard deviation. Position of FRT analyzed is indicated.

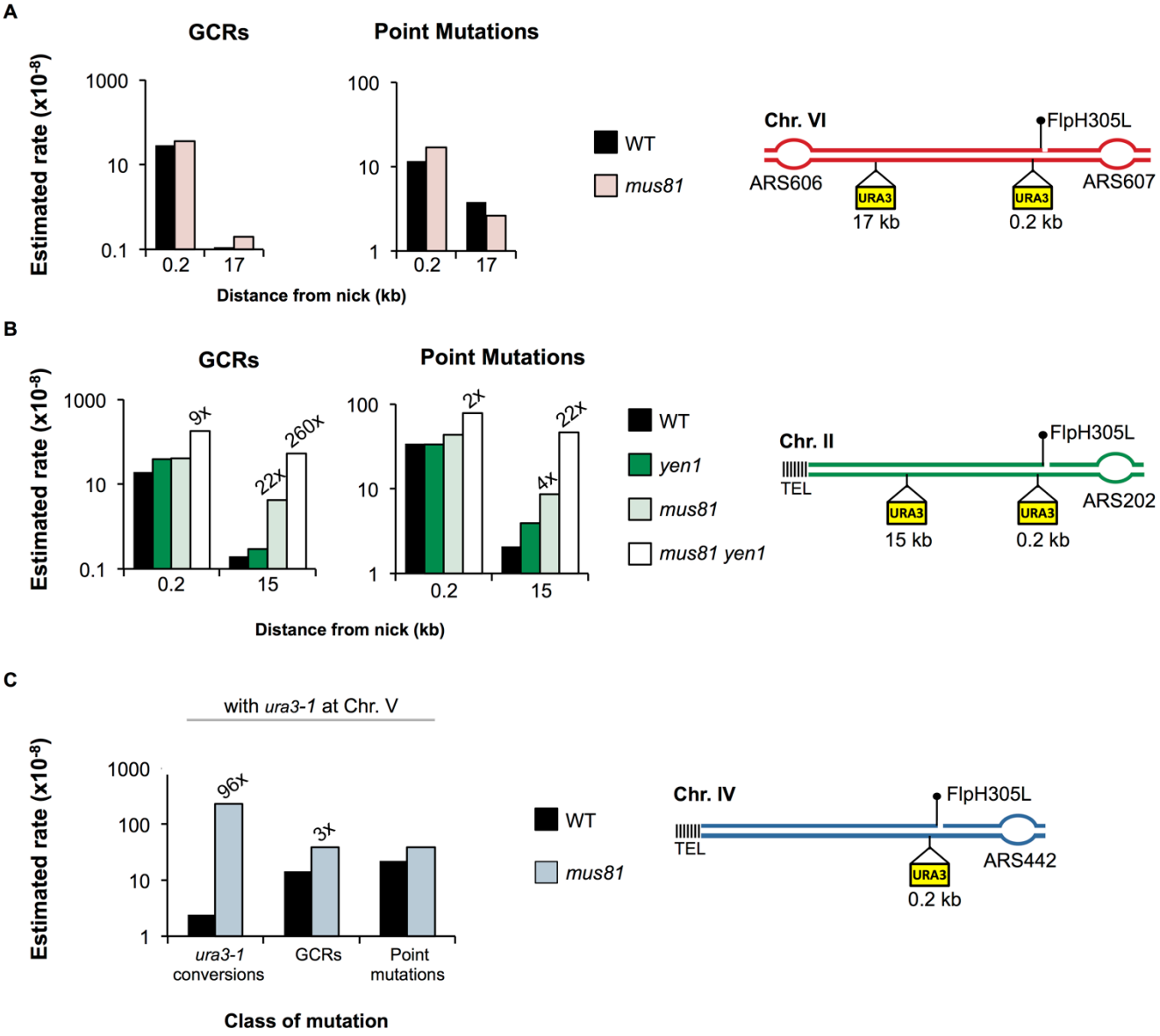

Fig. S5: Analysis of 5-FOA^R mutations

A-B. Estimated rates of GCRs and point mutations for *URA3* reporters on ChrVI (A) and ChrII (B), without the *ura3*-1 allele on ChrV. **C.** Estimated rates of *ura3-1* conversions, GCRs, and point mutations for the *URA3* reporter 0.2 kb from the FRT on ChrIV, for wild type and *mus81* cells. Fold changes above wild type are indicated.

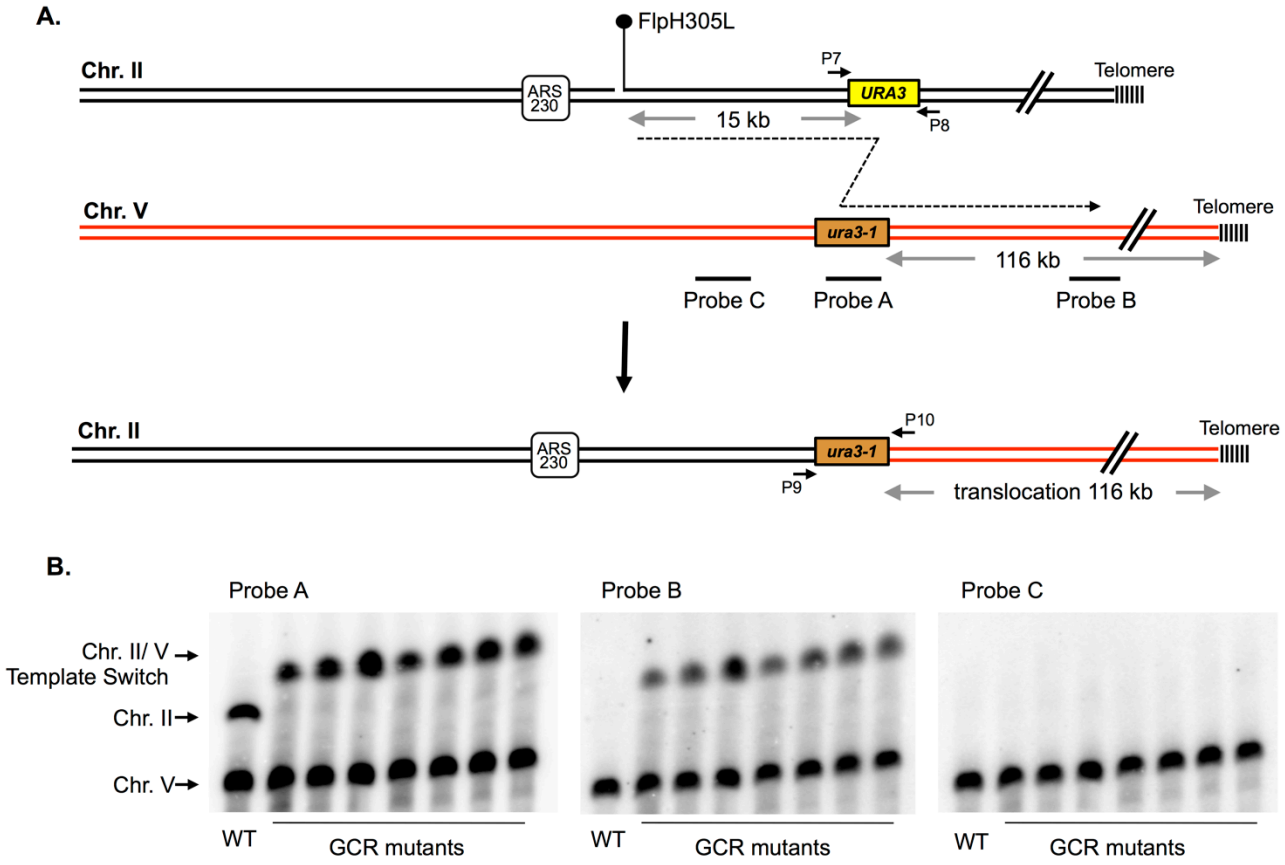

Fig. S6: *URA3/ura3-1* template switch mediated translocations between ChrII and ChrV in *mus81*Δ cells

A. A scheme showing the recombination event between ChrII and ChrV. Position of probes and PCR primers used for analysis are shown. **B**. Southern blot analysis of 7 template switch events using the indicated probes.

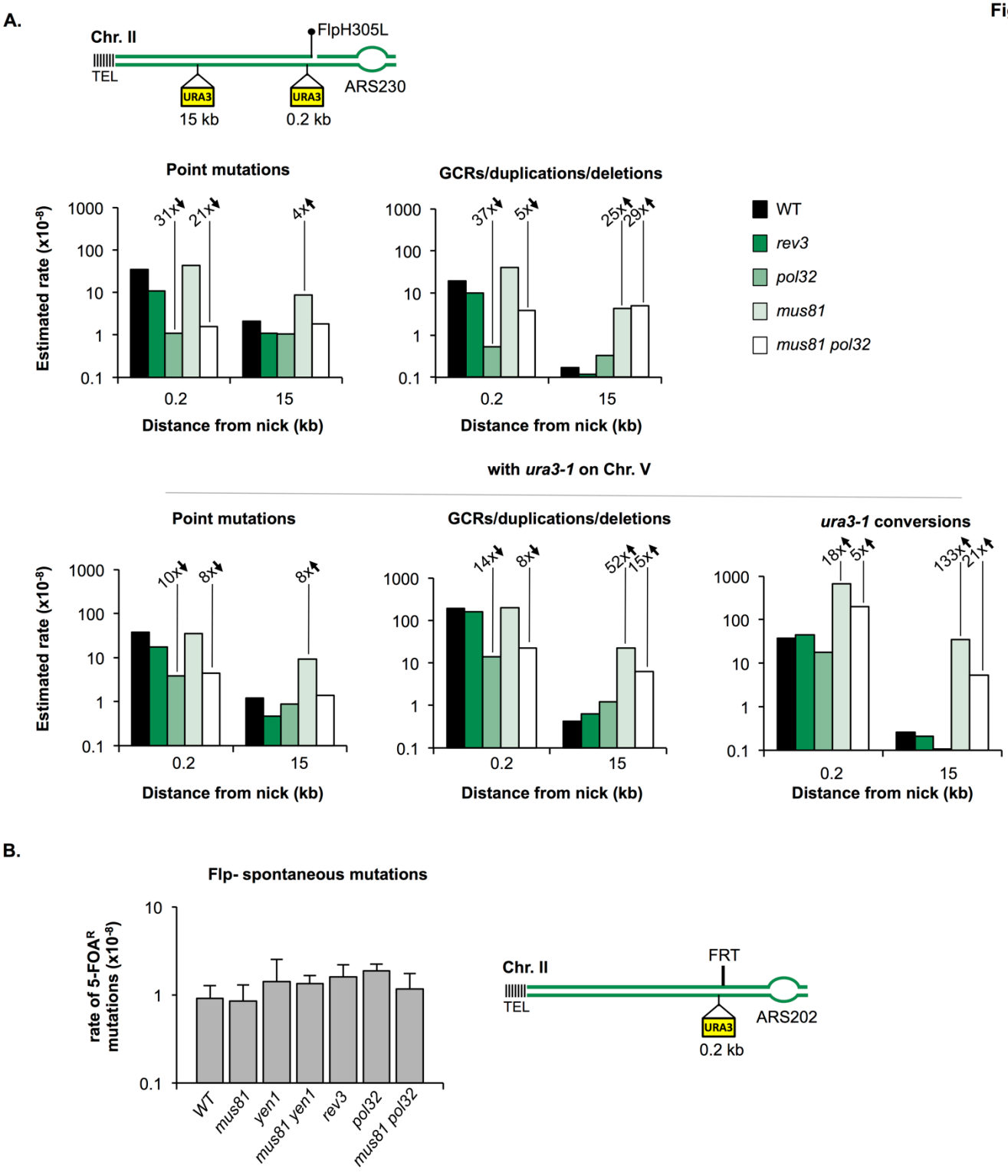

Fig. S7: Point mutations, template switches and GCRs at broken replication forks are mostly Pol32-dependent

A. Mutation spectrums in indicated mutant cells estimated for two positions on Chr II, either with or without *ura3-1* on Chr V. Fold changes relative to wild type at each position are indicated. **B.** Rates of spontaneous mutations measured as inactivation of the *URA3* reporter at ChrII-0.2 kb from the FRT site.

A.

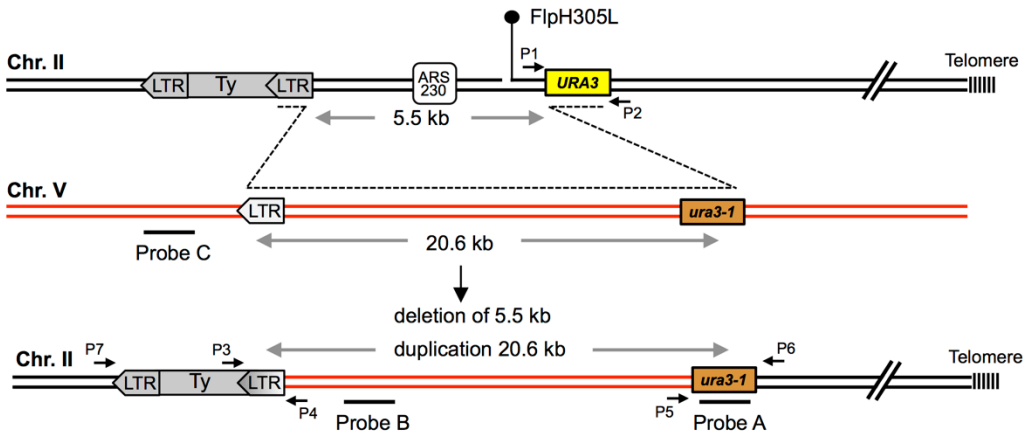

B.

# of tested FOA resistant colonies carrying GCR (*URA3* not amplified with P1/2)	LTR junctions amplified with P3/4 or P7/4, and *ura3-1* with P5/6 (lanes 2-5 below)	Only *ura3-1* junctions amplified with P5/6	Neither junction amplified
36	26	9	1

C.

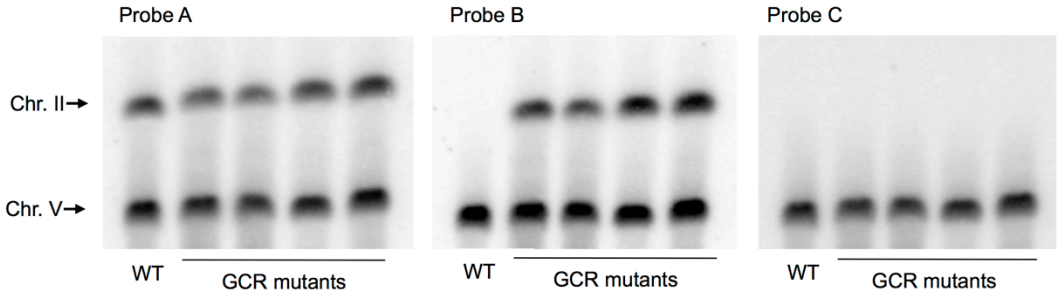

D.

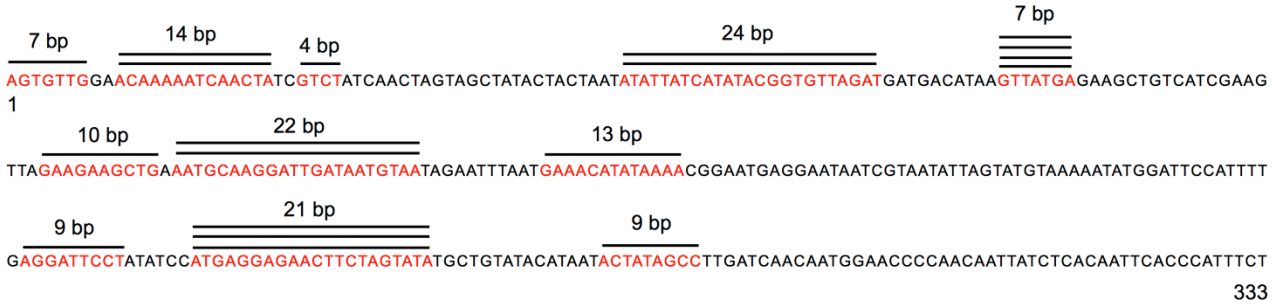

Fig. S8: Deletion-duplication rearrangement mediated by *URA3/ura3-1* and LTR repeats at ChrII and ChrV.

A. A scheme representing ChrII and ChrV participating in recombination. Position of diagnostic primer pairs for the *ura3-1* and LTR junctions and probes are indicated. The recombining LTRs on ChrII and ChrV share 79% sequence identity. **B.** Table describing the number of FOA resistant colonies tested for the deletion-duplication rearrangement. **C.** Southern blot analysis of 5 deletion-duplications, probes used indicated in (A). **D.** Sequence of LTR at ChrV is shown. Lines and red sequences indicate the homologous sequences at the LTR junction of ChrV and ChrII amplified with primers P3/4.

A.

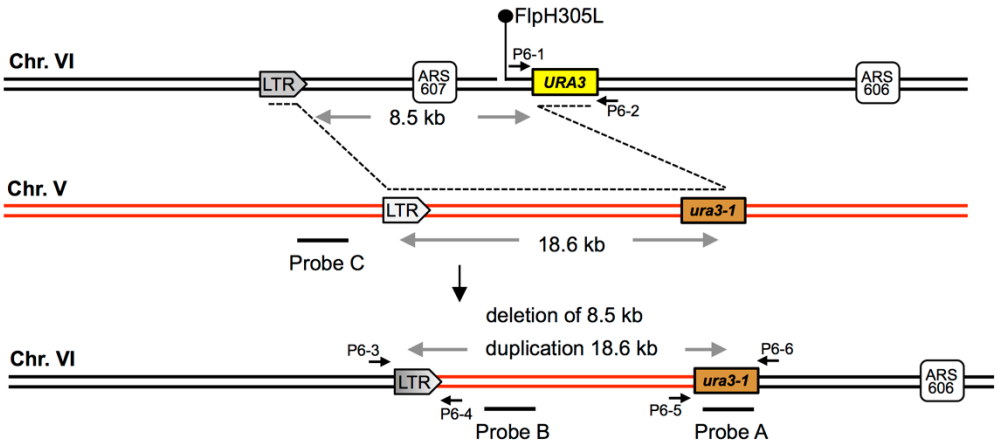

B.

# of tested FOA resistant colonies carrying GCR (*URA3* not amplified with P1/2)	LTR junctions amplified with P3/4 and *ura3-1* with P5/6 (lanes 3-5 below)	Only *ura3-1* junctions amplified with P5/6 (lane 2 below)	Neither junction amplified
10	4	2	4

C.

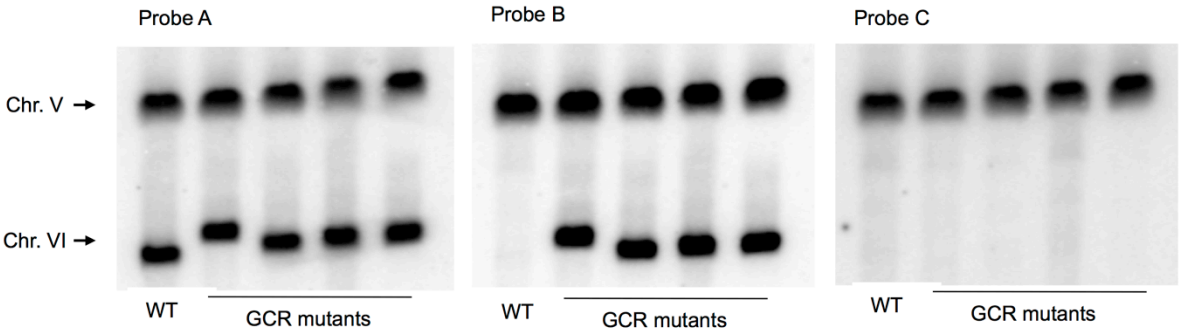

D.

GAGAATGTGGATTTTGATGTAATTGTTGGGATTCCATTGTGATTAAGGCTATAATATTAGGTATGTAGATATACTAGAAGTTCTCCTCGAGGATTTAGGAATCC
1

5 bp 7 bp 4 bp

ATAAAAGGGAATCTGCAATTCTACACAATTCTATAAATATTATTATCATCGTTTTATATGTTAATATTCATTGATCCTATTACATTATCAATCCTTGCGTTTCAGCTTCCACT

3 bp

AATTTAGATGACTATTTCTCATCATTTGCGTCATCTTCTAACACCGTATATGATAATATACTAGTAACGTAAATACTAGTTAGTAGATGATAGTTGATTTTTATTCCAACA

328

Fig. S9: Deletion-duplication rearrangement mediated by *URA3/ura3-1* and LTR repeats at ChrVI and ChrV.

A. A scheme representing ChrVI and ChrV participating in recombination. Position of diagnostic primer pairs for the *ura3-1* and LTR junctions and probes are indicated. The recombining LTRs on ChrVI and ChrV share 61% sequence identity. **B.** Table describing the number of FOA resistant colonies tested for the deletion-duplication rearrangement. **C.** Southern blot analysis of 5 deletion-duplications, probes used indicated in (A). **D.** Sequence of LTR at ChrV is shown. Lines and red sequences indicate the homologous sequences at the LTR junction of ChrV and ChrVI amplified with primers P6-3/6-4.

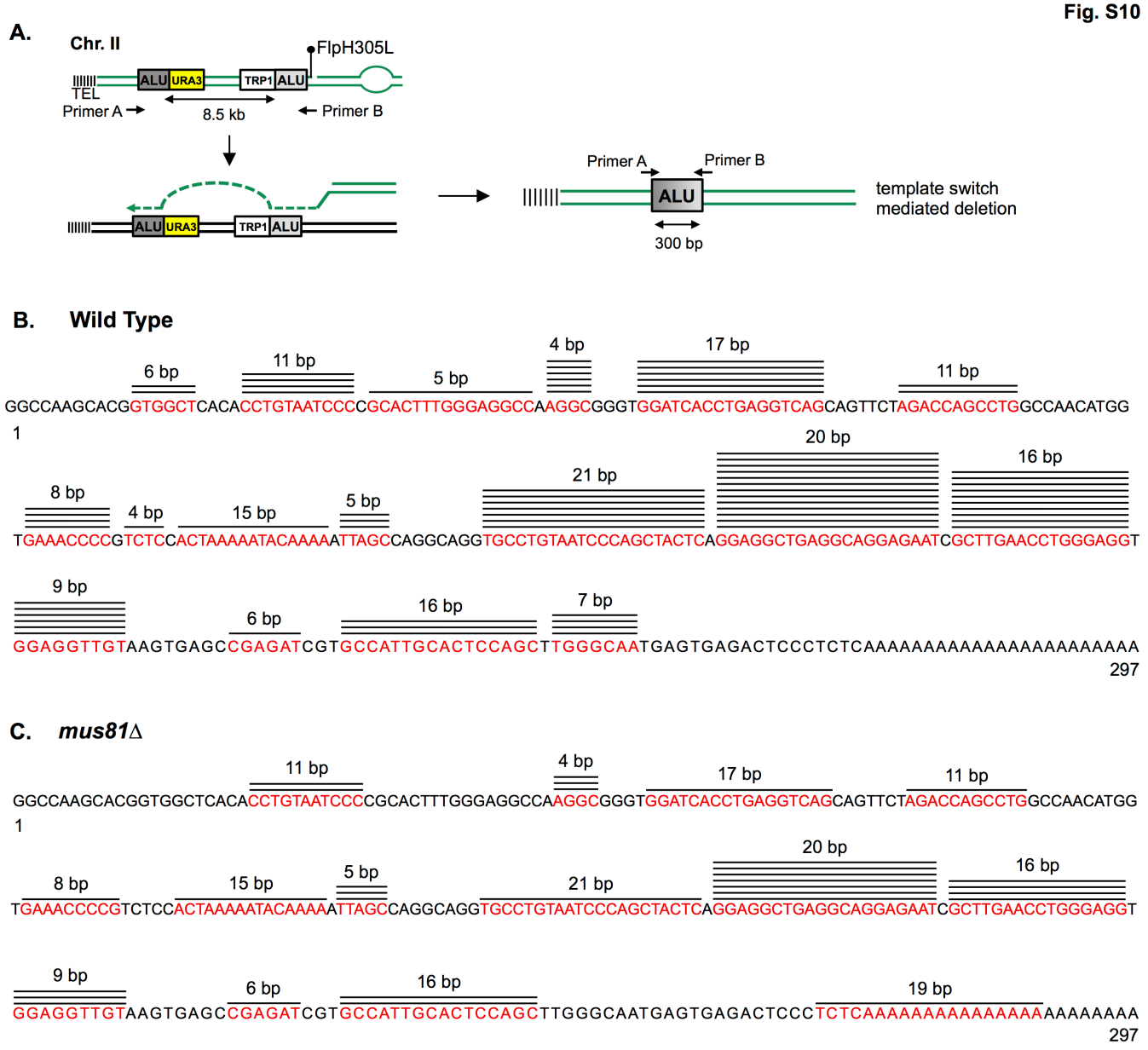

Fig. S10: Sequence analysis of *Alu-Alu* mediated template switches
A. A scheme showing *Alu* mediated template switches on ChrII. Locations of Primers A and B, used to amplify fusion *Alus* created by template switches, are indicated. **B-C.** Sequence of the telomere proximal *Alu* is shown. Red sequences and lines indicate homologous sequences used for template switches and the frequency of events observed.

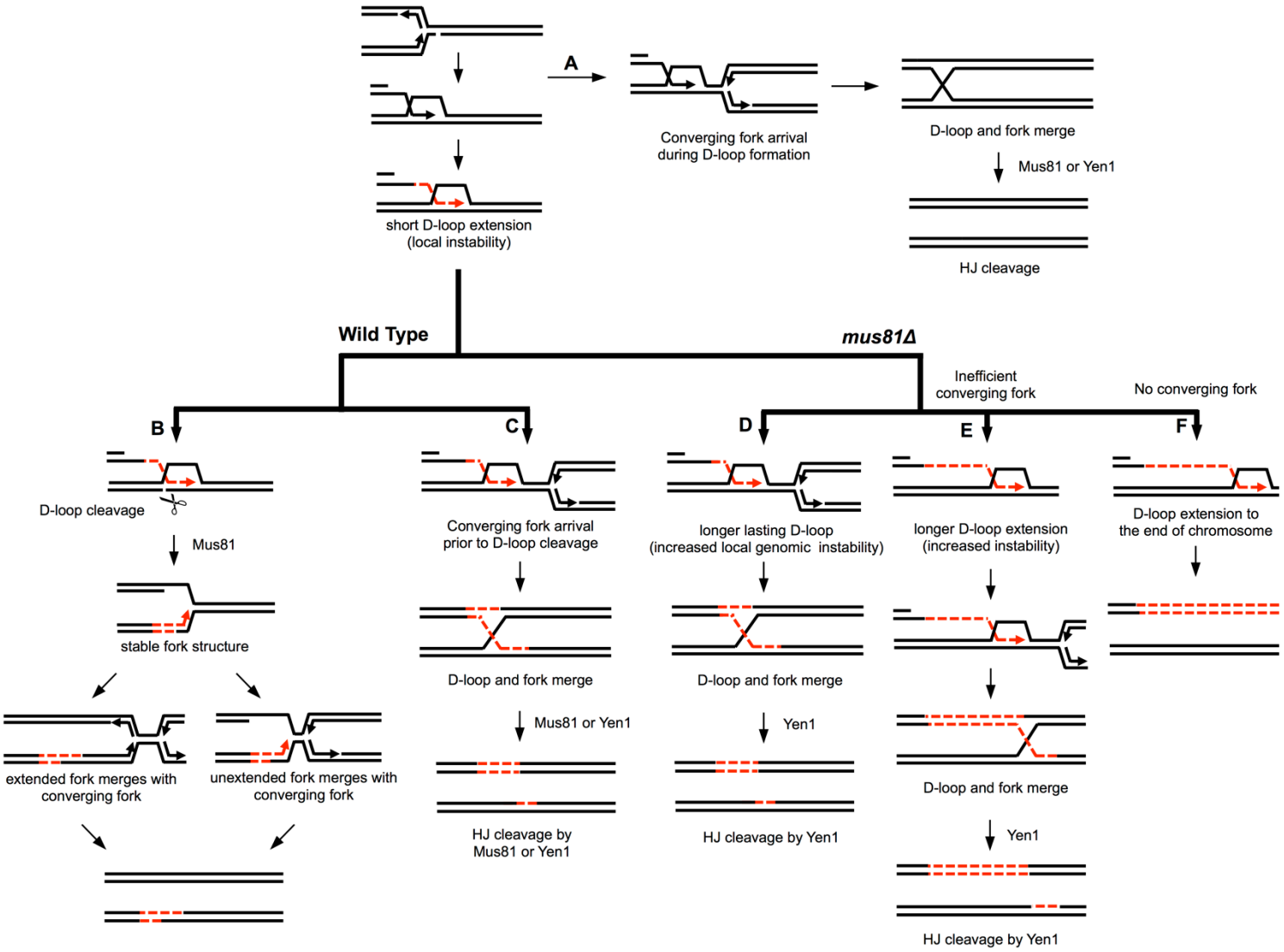

Fig. S11. **Comprehensive model for repair of broken replication forks**
Following fork breakage at a nick, a D-loop is formed. If a converging fork arrives at the time of D-loop formation, the two merge to form a HJ, which is cleaved by Mus81 or Yen1, and no mutagenic synthesis occurs (**A**). When the D-loop forms prior to converging fork arrival, the D-loop is initially extended by mutagenic BIR. In wild type cells, Mus81 can cleave the D-loop to form a stable fork structure and limit error prone synthesis. This fork structure can merge with a converging fork whether or not it is extended by a re-established replisome. Red dashed lines indicate mutagenic synthesis. (**B**). If a converging fork arrives prior to D-loop cleavage, the resulting sHJ can be cleaved by Mus81 or Yen1 (**C**). In *mus81* cells, the D-loop is longer lasting and can be extended a longer distance, particularly in the absence of an efficient converging fork (**D-E**), resulting in increased mutagenic synthesis. If an inefficient or dormant origin fires, the resulting converging fork will merge with the extending D-loop, resulting in a sHJ cleaved by Yen1 (**E**). If no converging fork is present, mutagenic BIR will proceed to the end of the chromosome (**F**).

	Genotype	FOA^R Rate (x10^{-8})	"Point Mutations" 1-2 nt Frameshifts	"Point Mutations" Base Subsititutions	"GCRs" 3-38 nt Duplications	"GCRs" Deletions	"GCRs" Other GCRs	*ura3-1* conversions	Total Mutants Analyzed
Chr II 0.2 kb	**WT**	54.2	14	19	1	1	17	**N/A**	52
	mus81	83.4	14	12		5	19	**N/A**	50
	yen1	73.1	13	9	1	5	20	**N/A**	48
	mus81yen1	260	8	9		11	28	**N/A**	56
	rev3	20.8	17	6	1	5	15	**N/A**	44
	pol32	1.6	13	17			15	**N/A**	45
	mus81pol32	5.4	6	9		17	17	**N/A**	49
	no FLP (spontaneous)	1.1	10	24			6	**N/A**	40
Chr II 0.2 kb	**WT**	266	3	4			36	7	50
with *ura3-1*	***mus81***	891	2	0		1	10	37	50
	yen1	304	1	1			38	10	50
	mus81yen1	1388	2	1		5	29	13	50
	rev3	515	1	3	2		34	10	50
	pol32	36.1	2	3			18	23	46
	mus81pol32	226	1			2	3	44	50
	no FLP (spontaneous)	0.9	5	25			1	9	40
Chr II 15 kb	**WT**	2.3	7	44	1		3	**N/A**	55
	mus81	12.9	9	25	1	5	11	**N/A**	51
	yen1	4.2	8	33	2		1	**N/A**	44
	mus81yen1	98.2	12	12		3	24	**N/A**	51
	rev3	1.2	5	23	1		2	**N/A**	31
	pol32	1.4	8	26		6	5	**N/A**	45
	mus81pol32	6.8	1	13	1	9	30	**N/A**	54
	no FLP (spontaneous)	1.6	5	33		1	1	**N/A**	40
Chr II 15 kb	**WT**	1.9	13	15	2	2	6	6	44
with *ura3-1*	***mus81***	66.4	3	4		2	15	26	50
	yen1	1.5	14	26	1		7	8	56
	mus81yen1	212	2	3		6	40	8	59
	rev3	1.3	3	10			18	6	37
	pol32	2.2	2	17		12	15	2	48
	mus81pol32	13.1	1	5		3	25	24	58
	no FLP (spontaneous)	0.9	6	24		1	5	5	41
Chr VI 0.2 kb	**WT**	40	8	8	3	2	34	**N/A**	55
	mus81	52.4	8	8		4	30	**N/A**	50
Chr VI 0.2 kb	**WT**	296	1	1		1	10	37	50
with *ura3-1*	***mus81***	1180	0	1			2	53	56
Chr VI 17 kb	**WT**	3.9	8	46		1		**N/A**	55
	mus81	2.7	13	38		1	2	**N/A**	54
Chr VI 17 kb	**WT**	3.4	10	13			7	17	47
with *ura3-1*	***mus81***	7.4	5	19				23	47
Chr IV 0.2 kb	**WT**	36.3	9	18		2	13	3	45
with *ura3-1*	***mus81***	307	2	4			6	36	48

Table S1: Mutations observed for FOA^R colonies

The number of observed mutations for each class from independent FOA^R colonies for each strain analyzed. Point mutations are further broken down into frame shifts or base substitutions and GCRs into duplications, deletions, or other rearrangements.